THE JOURNAL OF PHYSICAL CHEMISTRY A LETTERS

2007, *111,* 10020−10025
Published on Web 09/15/2007

The CN Stretching Band of Aliphatic Thiocyanate is Sensitive to Solvent Dynamics and Specific Solvation

Mark G. Maienschein-Cline and Casey H. Londergan*

Department of Chemistry, Haverford College, 370 Lancaster Avenue, Haverford, Pennsylvania 19041-1392

Received: July 31, 2007; In Final Form: August 23, 2007

Infrared absorption spectra in the C≡N stretching frequency region were collected for methyl thiocyanate, the simplest model aliphatic thiocyanate, in several common solvents to establish the dependence of the C≡N spectral band of aliphatic thiocyanate on its local solvation environment. Systematic changes in the C≡N bandwidth indicate that it reports on fast solvation dynamics. Anomalous asymmetry and temperature dependence of the C≡N band in fluorinated alcohol solvents indicates that these solvents participate in formation of a discrete hydrogen-bonded complex with the C≡N end of methyl thiocyanate. These observations indicate that the C≡N band of thiocyanate could be an effective site-specific probe of both specific hydrogen bonding and local dynamics in more complex systems, such as peptides and proteins.

Introduction

The responses of single molecular vibrations to changes in the local environment have been noted in a variety of condensed-phase systems. In particular, the C≡N stretching vibration of nitrile groups has been shown to be a sensitive reporter of the local electrostatic and hydrogen-bonding environment.[1−4] This sensitivity has been used recently to report on features of the structural environment of 4-cyanophenylalanine[5] in several different contexts,[6,7] with the goal of observing peptide and protein structure via infrared spectroscopy on a single-site basis. Unlike single-site peaks in NMR spectroscopy, single vibrational band profiles can provide a direct probe of both the local structural distribution and the solvation environment, including fast dynamics. The C≡N stretching bands are especially useful in peptide contexts since they absorb in a relatively uncluttered region of the infrared spectrum and can be clearly observed in H_2O solutions.

A C≡N stretching band of new interest[8] in such contexts is that of aliphatic thiocyanate, which can be introduced using established synthetic protocols[9,10] by selective functionalization of free cysteine side chains. By varying the solvent, the current work demonstrates the sensitivity of the C≡N stretching band of a simple aliphatic thiocyanate, methyl thiocyanate, to its local environment. Extinction coefficients, band frequencies, and line shapes are analyzed as a function of different characteristics of the solvent. A systematic understanding of the variation of the spectral appearance of the C≡N stretching band is necessary to understand its behavior in more complicated condensed-phase systems, including chemically modified peptides and proteins.

Experimental Methods

Methyl thiocyanate was used as received from Acros. Double-deionized milli-Q quality water was used for the aqueous sample. All other solvents were HPLC or spectrophotometric grade from Aldrich and used as received.

Mid-infrared absorption spectra were collected from 4000 to 1000 cm^{-1} on a Bruker Vertex 70 FT-IR spectrometer, using 256 scans per sample, with a resolution of 2 cm^{-1}. Samples were mounted in a Harrick demountable liquid cell with calcium fluoride salt plates and a Teflon spacer; a 25 μm path length spacer was used for samples in aqueous solution and alcohol solutions, and a 100 or 150 μm path length was used for samples in other organic solvents. Organic solvent solutions were injected into the IR cell in a flow-cell geometry using built-in Luer ports; aqueous solutions were pipetted onto the plates of the open cell. All spectra shown here have been background-subtracted using a background spectrum of pure solvent. Extinction coefficients were calculated as the slope of a linear fit to a graph of absorption peak height versus path length times concentration at four different concentrations. Line shape analysis was performed using Microcal Origin 7.1 (see details below).

Temperature-dependent spectra were collected using a Harrick temperature-controlled demountable liquid cell with the same materials and loading procedure as that above; the temperature was controlled using a Thermo-Neslab circulating bath with 20% ethylene glycol in deionized water as the circulating fluid.

Normal-mode analysis was performed using Gaussian98;[11] the density functional B3LYP[12,13] was used with the 6-31G** basis set on all atoms. Predicted vibrational frequencies were all within 5% of frequencies evident in the infrared absorption spectrum.

Results and Discussion

The normalized C≡N stretching spectra for MeSCN in nine different solvents are shown in Figure 1. Note that although no two bands lie directly on top of each other, the bands all appear within a relatively narrow spectral region. All bands appear symmetric in shape except for the bands in fluorinated alcohols; these bands are distinct in both frequency and band shape. These

* To whom correspondence should be addressed. E-mail: clonderg@haverford.edu.

10.1021/jp0761158 CCC: $37.00 © 2007 American Chemical Society

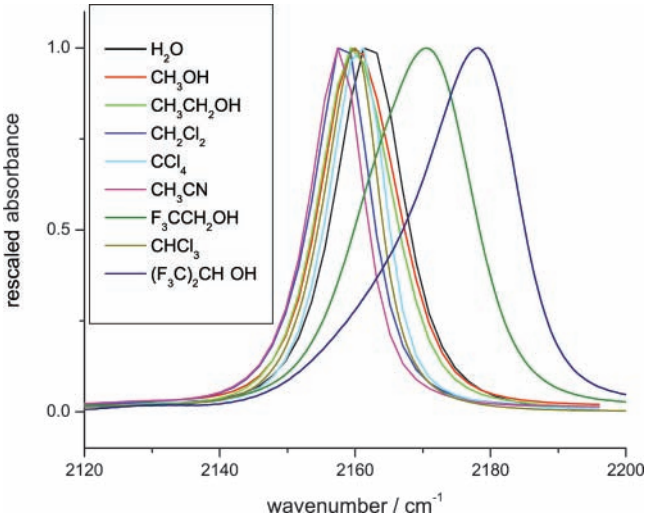

Figure 1. C≡N stretching absorption bands for methyl thiocyanate in several common solvents.

spectra will be treated separately below. Calculated parameters for each stretching band are presented in Table 1, along with solvent dielectric constants and previously established dynamic solvent parameters.

Extinction Coefficient and Central Frequency. The extinction coefficient for MeSCN varies with solvent, but not systematically with dielectric constant and not over a very large range compared to some nitriles (up to a factor of 2). Both the lowest and highest extinction coefficients observed are in alcohol solvents; thus, it appears unlikely that the extinction coefficient is a systematic reporter of hydrogen bonding. Central frequencies vary only from 2157 to 2162 cm^{-1} in non-fluorinated solvents, and they do appear to depend slightly on the hydrogen-bonding character of the solvent, with the weak trend that the highest frequencies are observed in H-bonding solvents and the lowest frequencies in non-H-bonding solvents. The band frequency does not depend systematically on solvent dielectric constant.

Line Shape and Solvent Dynamics. Symmetric C≡N stretching bands were fitted to the following pseudo-Voigt linear combination of a Gaussian and a Lorentzian frequency distribution

$$y_0 + A\left(m_{\text{Lorentz}}\frac{2}{\pi}\frac{\text{FWHM}}{4(\tilde{\nu}-\tilde{\nu}_c)^2+\text{FWHM}^2}+ (1-m_{\text{Lorentz}})\frac{\sqrt{4\ln 2}}{\sqrt{\pi}\text{FWHM}}\exp\left[-\frac{4\ln 2}{\text{FWHM}^2}(\tilde{\nu}-\tilde{\nu}_c)^2\right]\right)$$

where FWHM is the full-width at half-maximum of both the Lorentzian and Gaussian distributions (and thus always the full-width at half-maximum of the observed band); m_{Lorentz} is the fraction of Lorentzian character (thus $m_{\text{Lorentz}} = 1$ would denote a fully Lorentzian band shape, and $m_{\text{Lorentz}} = 0$ would lead to a fully Gaussian band shape); A is an amplitude parameter, and y_0 is a baseline offset; and $\tilde{\nu}_c$ is the central band frequency. The experimental parameter FWHM and the fitted parameter m_{Lorentz} appear in Table 1; note that because the pseudo-Voigt profile is a symmetric function around $\tilde{\nu}_c$, fits to spectra in fluorinated alcohols are not reported since these fits would not be accurate representations of the absorption line shapes. The experimental width of the symmetric C≡N bands varies depending on the solvent between approximately 8.5 and 13.2 cm^{-1} and appears to vary systematically with different solvent types.

The fitted parameters m_{Lorentz} and FWHM could reflect solvation dynamics in the following simple way. Assuming that the only Gaussian contributions to the frequency distribution are inhomogeneous, m_{Lorentz} would increase as the spectral diffusion time scale of the frequency distribution speeds up. At the same time, FWHM should decrease due to increased dynamic averaging out of the inhomogeneous distribution of frequencies. Thus, if a dependence of line shape on fast solvent dynamics were to be observed, more Lorentzian C≡N stretching bands would also be narrower. One way to quantify this is to calculate FWHM/m_{Lorentz}; this quantity should decrease as the solvent response time decreases. The tacitly assumed model here is Bloch dynamics; however, dynamic band narrowing in a more complicated model would lead to qualitatively similar effects on the spectral bandwidth. FWHM/m_{Lorentz} for each band is included in Table 1. For comparison, also included in Table 1 is the average solvation time $\langle\tau\rangle$ of Maroncelli and co-workers,[14] determined using time-resolved Stokes shifts of coumarin 153. Values of $\langle\tau\rangle$ are not reported for CCl_4 and water because these solvents were not reported by Horng et al.; subsequent experiments by other groups[15,16] indicate substantial qualitative differences between the dipolar solvation response of water and that of other solvents.

There is a clear dependence of the C≡N line shape on solvent dynamics. In Table 1, as FWHM/m_{Lorentz} decreases, there is a decrease in $\langle\tau\rangle$. This method of line shape analysis clearly identified acetonitrile as the "fastest" solvent and ethanol as the "slowest" solvent (of those comparable to $\langle\tau\rangle$ values). This line shape analysis appears to be most sensitive to differences between the "fastest" solvents and less so to the differences between, for example, methanol and ethanol. There are certainly other contributing factors to the line width, some from bulk effects and rotational time of the solute molecule. A similar study was undertaken some time ago by Higuchi et al.[17] to examine these effects, with the conclusion that viscosity and solvent molecular weight play only minor roles in determining the spectral bandwidth; in light of more recent understanding of solvent dynamics at fast time scales, their data (albeit without the line shape analysis performed here) are remarkably consistent with the assertion that fast solvent dynamics plays an important role in determining both the width and shape of the C≡N stretching band.

The relatively rigid structure of the solute MeSCN suggests that the inhomogeneous distribution of frequencies in each case here should derive mainly from differences in the configuration of solvent molecules around the solute molecule, specifically at the C≡N end of the molecule. The fact that the C≡N stretching bandwidth and line shape report on the fast dynamics of this solvent configuration is not particularly surprising, but it could be quite useful in observing subtle differences between the environments of modified cysteine residues located in specific regions of peptides and proteins. The symmetry of the C≡N bands in the first seven solvents in Table 1 suggests that there are no specific solvent configurations around MeSCN which are thermodynamically favored in these solvents.

Line Shape in Fluorinated Alcohols. However, the bands observed in the fluorinated alcohols trifluoroethanol (TFE) and hexafluoroisopropanol (HFIP) are markedly asymmetric and do not fit to a single frequency distribution. Fitting to multiple Gaussians indicates that the C≡N band in TFE can be fitted using two Gaussians, while the C≡N band in HFIP cannot be easily fitted to fewer than three Gaussian bands. Careful experiments over several orders of magnitude in MeSCN concentration indicate that the C≡N line shapes in these solvents

TABLE 1: Experimentally Determined and Fitted Parameters for the CN Absorption Band of Methyl Thiocyanate in Different Solvents

solvent	ϵ/ $cm^{-1}M^{-1}$	central frequency/ cm^{-1}	dielectric constant	FWHM/ cm^{-1}	$m_{Lorentz}$	FWHM/$m_{Lorentz}$/ cm^{-1}	$\langle\tau\rangle$/ (ps)
MeCN	115.5	2157.2	36.6	8.45	0.994	8.50	0.26
CH_2Cl_2	94.3	2157.6	8.9	10.3	0.729	14.13	0.56
$CHCl_3$	125.4	2159.2	4.9	10.03	0.70	14.33	2.8
CCl_4	79.4	2160.0	2.2	10.13	0.569	17.8	*a*
MeOH	86.8	2160.5	32.6	13.23	0.652	20.29	5.0
EtOH	88.5	2160.1	24.6	11.83	0.526	22.49	*a*
H_2O	153.8	2162.0	78.4	12.81	0.554	23.12	16
HFIP	161.2	2178	16.7				
TFE	163.6	2171	26.5				

[a] Values for these solvents were not reported by Horng et al.

do not change significantly with concentration; therefore, the asymmetry is not from intersolute or clustering effects. Several nitriles and organic cyanates display Fermi resonances between C≡N stretching bands and linear combinations of lower-frequency bands;[3,18] this is likely not the case for MeSCN. Normal-mode analysis indicates that there are no low-frequency modes (for example, the SCN bending motion and the C−S stretch) whose motions could easily come into Fermi resonance with the C≡N stretching mode. The strongly temperature-dependent behavior (see below) of these band shapes also does not match that expected if the anomalous band shapes were due to Fermi resonance with lower-frequency normal modes whose excited-state populations change significantly with temperature.

The temperature dependence of the C≡N stretching bands of MeSCN in TFE and HFIP was determined to ascertain whether the line shape asymmetry at room-temperature could arise from specific solvation effects (i.e., a discrete number of preferred solvent configurations). Temperature-dependent spectra for TFE and HFIP are shown in Figure 2a and b. There is a clear temperature dependence of the C≡N stretching profile in each fluorinated alcohol solvent. The general trend in each spectrum as the temperature increases is toward a broader, more symmetric line shape centered at lower frequency.

The spectrum in TFE at all temperatures (Figure 2a) fits well to a linear combination of two Gaussian bands centered at 2172.9 and 2164.9 cm^{-1} with respective widths (full-width at half-maximum) of 14.5 and 18.7 cm^{-1}; see Table 2 for fits at all temperatures for TFE. As the temperature increases, the amplitude of the lower-frequency component increases at the expense of the higher-frequency component's amplitude. This analysis suggests that the spectrum of MeSCN in TFE is made up of two subpopulations; these subpopulations could be due to different hydrogen-bond conformers at the C≡N end of the solute molecule. No dynamics are taken into account in this treatment; the fit of the spectrum to two subpopulations at all temperatures suggests that the dynamics of exchange between subdistributions are slower than the infrared line shape could detect.

The line shape in HFIP, however, has a more pronounced low-frequency tail than does the line shape in TFE and does not fit well to two Gaussians. The trend with temperature is similar to that in TFE but at no point is the spectrum as simply analyzed as that in TFE. To recover information on underlying subpopulations in both the TFE and HFIP spectra, two-dimensional correlation analysis was performed on each set of temperature-dependent spectra following the well-established procedure of Noda[19] (see Supporting Information for details of analysis). Synchronous and asynchronous correlation maps for the data in Figure 2 are shown in Figure 3.

The interpretation of the synchronous correlation maps (Figure 3A−B) is straightforward. In synchronous correlation maps, diagonal peaks appear where spectral intensity changes, and off-diagonal peaks indicate by their sign whether the spectral changes associated with the diagonal peaks change together or at the expense of each other. The synchronous maps for the TFE and HFIP data are similar: a region of spectral change is observed at high frequency; in HFIP, a change is observed at lower frequency as well. A negative cross peak appears in each synchronous map between the high- and low-frequency regions. This indicates that changes on the high- and low-frequency sides of the C≡N stretching bands occur at the expense of each other in a correlated fashion. In HFIP, the negative off-diagonal correlation peaks are elongated; the simplest interpretation of these features is that the temperature-dependent spectra in HFIP indicate an exchange of population between two main subdis-

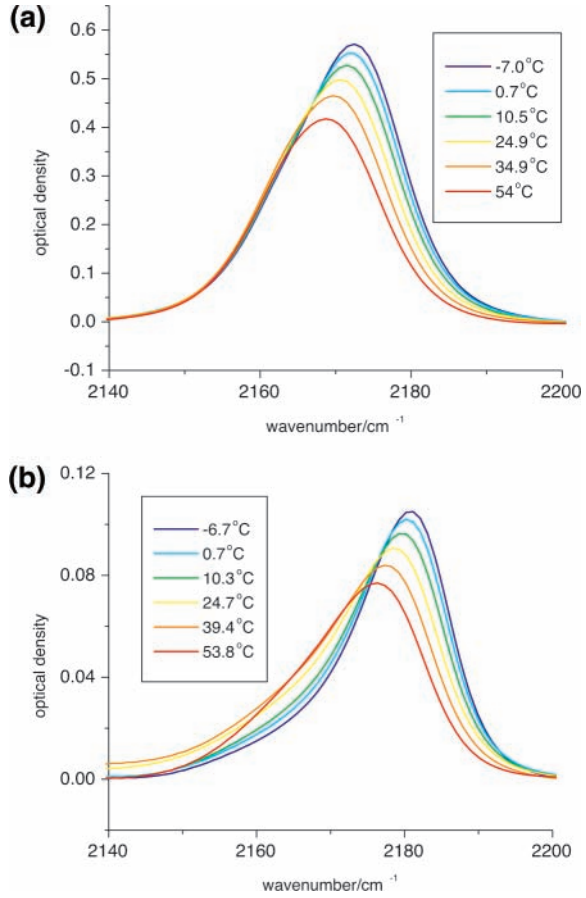

Figure 2. Temperature-dependent CN stretching bands for methyl thiocyanate in fluorinated alcohols; (a) trifluoroethanol, (b) hexafluoroisopropanol.

TABLE 2: Fitted Amplitude Parameters for Global Fitting of the Temperature-Dependent CN Stretching Spectra of MeSCN in TFE (Figure 2A)[a]

temperature (°C)	A_1	A_2
−7	0.45	0.18
0.7	0.41	0.20
10.5	0.37	0.23
24.9	0.31	0.26
39.4	0.25	0.28
54.0	0.18	0.29

[a] A_1 is the amplitude of a Gaussian band at 2172.9 cm^{-1} with a FWHM of 14.5 cm^{-1}; A_2 is the amplitude of a Gaussian band at 2164.9 cm^{-1} with a FWHM of 18.7 cm^{-1}.

tributions, one at high frequency with a relatively symmetric shape and one at lower frequency with a more asymmetric shape and a long low-frequency tail. These two subpopulations compete thermodynamically with each other, with the high-frequency population being more stable.

The interpretation of the asynchronous correlation maps (Figure 3C−D) is less straightforward. There are no diagonal peaks in asynchronous maps; off-diagonal peaks occur between changing spectral features that are not correlated with each other. An important first observation for the TFE and HFIP data is that all features in the calculated asynchronous maps are much weaker (less than 1/10 of the intensity) than the features in the corresponding synchronous maps. This weakness of features indicates that the observed spectral changes are largely due to correlated processes. The simple asynchronous map for the TFE spectra (Figure 3C) indicates that some small uncorrelated spectral changes occur along the spectral length of the C≡N band without any specific features standing out. The shape of the TFE map is in full agreement with the above assertion that the TFE spectra display the temperature-selective population of two subdistributions. The shape of the TFE asynchronous map matches the expectation from the paradigmatic case of two overlapping bands.[20] However, the more complicated asynchronous map for the HFIP spectra (Figure 3D) indicates that more than two subdistributions may be present in the spectrum and, further, that these underlying subdistributions change with temperature in a more complicated way. The shape of the main spectral features does not match the simple case of two overlapping bands; the distorted shape of the most intense asynchronous bands may be due to band broadening with temperature. The presence of more asynchronous features than those in the TFE asynchronous map indicates a more complicated, yet still discrete, number of subdistributions underlying the envelope of the C≡N stretching absorption band in HFIP.

Although the features of the asynchronous correlation maps for MeSCN in these two solvents are qualitatively different, the temperature-dependent spectra share the common elements of a high-frequency band which is mainly populated at low temperature and a lower-frequency band or group of bands which is mainly populated at higher temperature. As the nitrile C−C≡N moiety accepts a H-bond, its frequency typically shifts to higher wavenumber.[2] For thiocyanate, the frequency shift with hydrogen bonding at N has also been shown to lead to an increase in frequency.[21,22] Most previous work investigating the effect of H-bonding and solvent association with thiocyanates has been performed with SCN^- salts; the current work is more topical to the possible extension of these observations in any system containing aliphatic thiocyanates, including thiocyanatoalanine residues in peptides.

The spectral shapes observed here are most likely due to specific spectral effects of H-bonding; the two subpopulations are assigned as H-bonded SC≡N (high frequency) and non-H-bonded SC≡N (low frequency), in accordance with assignments for SCN^- in H-bonding solvents. The trend observed with changing temperature here is qualitatively similar to that observed for the C≡N group of 4-cyanophenylalanine in water;[2] in the data for MeSCN in fluorinated alcohols, the high-frequency region is depopulated at high temperature, while for cyanophenylalanine in water, the average band frequency is lower at higher temperatures. However, line shape differences in the high- and low-temperature limits indicate that the relative stability and number of specifically solvated complexes for MeSCN in fluorinated alcohols is different than that for cyanophenylalanine in water.

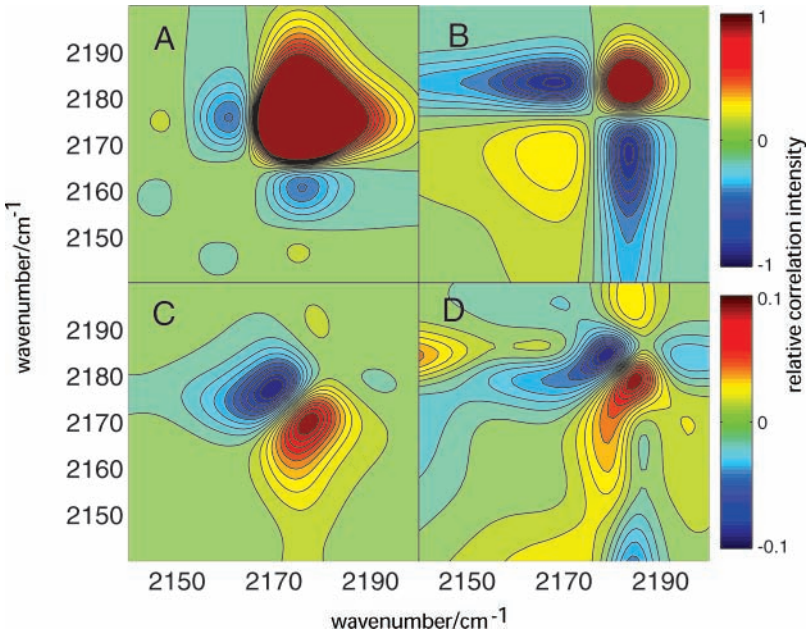

Figure 3. Two-dimensional correlation contour maps for temperature-dependent changes in the absorption spectra of MeSCN in fluorinated alcohols. (A) Synchronous correlation map for TFE. (B) Synchronous correlation map for HFIP. (C) Asynchronous map for TFE. (D) Asynchronous map for HFIP. Relative contour levels are shown at the right. Contour levels for asynchronous maps are roughly 1/10 of those for the synchronous maps.

The data reported here indicate that there is a specific H-bonded complex formed between the nitrogen end of MeSCN and fluorinated alcohols which becomes less thermodynamically favored as the temperature increases. Specific H-bonded complexes of the thiocyanate anion with alcohols are well-known.[21,22] The fluoroalcohol/NCS−Me H-bonded complex observed here has a different characteristic C≡N stretching frequency and thus a different strength of H-bonding in TFE versus that in HFIP; furthermore, this complex is not observed for MeSCN in any other solvents, even those capable of H-bonding. The broader low-frequency distribution corresponds to non-H-bonded, nonspecifically solvated species. The asymmetry of the non-H-bonded, low-frequency part of the spectrum in HFIP suggests that some additional specific solvation effects may participate in the "non-H-bonded" solvation environments in HFIP.

Specific Solvation versus Dynamics. The observation of what is likely specific solvation through H-bonding of the C≡N moiety of aliphatic thiocyanate by fluorinated alcohols suggests that modified cysteine could be a clear and site-specific probe of the "dehydration" effects of these solvents on peptides.[23,24] Both TFE and HFIP are used routinely to "force" helical structure in peptides and proteins which may be conformationally, but not thermodynamically, predisposed to adopting a helical secondary structure. The hypothetical basis for this helix-forcing ability is dehydration of the peptide backbone through specific solvation and replacement of H-bonds between water and the peptide backbone with stronger fluoroalcohol H-bonds. Local clustering of fluorinated alcohol molecules near easily dehydrated sequences is likely in this scenario. The C≡N stretch of modified cysteine could be a very sensitive probe of the presence of fluorinated alcohol molecules in the vicinity of chosen peptide residues, and thus, it could help to elucidate the molecular action of "the TFE effect" in specific regions of peptides where fluorinated alcohol molecules tend to cluster. Non-fluorinated alcohols and water appear not to form H-bonded complexes with MeSCN; however, more indirect effects of their interaction with the CN end of the solute molecule are evident in the small positive frequency shift observed in these weaker H-bond donor solvents as compared to that of the non-H-bonding solvents.

The C≡N stretching spectra of MeSCN in TFE and HFIP exhibit effects of specific interactions of a piece of the probe molecule with a single solvent molecule. The symmetric bands observed in other solvents suggest a lack of such specificity of interaction. In the solvents without evidence of specific H-bonding interactions, the line shape depends on the characteristic reorganization time scale of the local environment. In TFE and HFIP, there are also likely small dynamic exchange effects which contribute to the spectrum; there must be a characteristic time scale for the exchange of the H-bonded species with the non-H-bonded distribution. Features of the dynamics associated with both line narrowing in the nonspecifically solvated species and exchange between H-bonded and non-H-bonded species could be discovered through recently achieved nonlinear vibrational spectroscopy experiments.[25,26] Such interrogation could also confirm the assertions of this letter. Since the C≡N frequency does appear to depend to some extent on H-bonding activity even when specific complexes are not observed, time-resolved echo experiments which monitor the spectral diffusion dynamics of the C≡N stretching band would be expected to indicate more subtle and complicated differences in local solvent dynamics than are possible through analysis of absorption line shapes.

Conclusions

Regardless of higher-order experiments (which are underway), the data presented here indicate that the C≡N stretching mode of aliphatic thiocyanate is quite sensitive to particular dynamic and H-bonding properties of its local environment. This suggests that the C≡N stretching band of thiocyanatoalanine (modified cysteine) should be a very useful dynamic and specific probe of its local environment when incorporated in proteins. The main points here are that fluorinated alcohols form specific H-bonded complexes with aliphatic thiocyanate and that if no specific complexes are formed, the CN line shape depends on the dipolar reorientation dynamics of the solvent. Further experiments are in progress in model peptide systems to demonstrate the sensitivity of this vibrational probe to both specific structural features of the local environment, such as H-bond donor groups, and nonspecific dynamic features like relaxation and fluctuation of both the local solvent and the local structure.

Acknowledgment. C.H.L. gratefully acknowledges support from Haverford College and from the Camille and Henry Dreyfus Foundation (New Faculty Start-Up Award).

Supporting Information Available: Description of the calculations of the two-dimensional contour maps. This material is available free of charge via the Internet at http://pubs.acs.org.

References and Notes

(1) Fawcett, W. R.; Liu, G. J.; Kessler, T. E. *J. Phys. Chem.* **1993**, *97*, 9293.

(2) Huang, C. Y.; Wang, T.; Gai, F. *Chem. Phys. Lett.* **2003**, *371*, 731.

(3) Nyquist, R. A. *Appl. Spectrosc.* **1990**, *44*, 1405.

(4) Reimers, J. R.; Hall, L. E. *J. Am. Chem. Soc.* **1999**, *121*, 3730.

(5) Getahun, Z.; Huang, C. Y.; Wang, T.; De Leon, B.; DeGrado, W. F.; Gai, F. *J. Am. Chem. Soc.* **2003**, *125*, 405.

(6) Tucker, M. J.; Getahun, Z.; Nanda, V.; DeGrado, W. F.; Gai, F. *J. Am. Chem. Soc.* **2004**, *126*, 5078.

(7) Schultz, K. C.; Supekova, L.; Ryu, Y. H.; Xie, J. M.; Perera, R.; Schultz, P. G. *J. Am. Chem. Soc.* **2006**, *128*, 13984.

(8) Fafarman, A. T.; Webb, L. J.; Chuang, J. I.; Boxer, S. G. *J. Am. Chem. Soc.* **2006**, *128*, 13356.

(9) Degani, Y.; Neumann, H.; Patchornik, A. *J. Am. Chem. Soc.* **1970**, *92*, 6969.

(10) Degani, Y.; Patchornik, A. *Biochemistry* **1974**, *13*, 1.

(11) Frisch, M. J.; Trucks, G. W.; Schlegel, H. B.; Scuseria, G. E.; Robb, M. A.; Cheeseman, J. R.; Montgomery, J. A., Jr.; Vreven, T.; Kudin, K. N.; Burant, J. C.; Millam, J. M.; Iyengar, S. S.; Tomasi, J.; Barone, V.; Mennucci, B.; Cossi, M.; Scalmani, G.; Rega, N.; Petersson, G. A.; Nakatsuji, H.; Hada, M.; Ehara, M.; Toyota, K.; Fukuda, R.; Hasegawa, J.; Ishida, M.; Nakajima, T.; Honda, Y.; Kitao, O.; Nakai, H.; Klene, M.; Li, X.; Knox, J. E.; Hratchian, H. P.; Cross, J. B.; Bakken, V.; Adamo, C.; Jaramillo, J.; Gomperts, R.; Stratmann, R. E.; Yazyev, O.; Austin, A. J.; Cammi, R.; Pomelli, C.; Ochterski, J. W.; Ayala, P. Y.; Morokuma, K.; Voth, G. A.; Salvador, P.; Dannenberg, J. J.; Zakrzewski, V. G.; Dapprich, S.; Daniels, A. D.; Strain, M. C.; Farkas, O.; Malick, D. K.; Rabuck, A. D.; Raghavachari, K.; Foresman, J. B.; Ortiz, J. V.; Cui, Q.; Baboul, A. G.; Clifford, S.; Cioslowski, J.; Stefanov, B. B.; Liu, G.; Liashenko, A.; Piskorz, P.; Komaromi, I.; Martin, R. L.; Fox, D. J.; Keith, T.; Al-Laham, M. A.; Peng, C. Y.; Nanayakkara, A.; Challacombe, M.; Gill, P. M. W.; Johnson, B.; Chen, W.; Wong, M. W.; Gonzalez, C.; Pople, J. A. *Gaussian 03*, revision B.04; Gaussian, Inc.: Pittsburgh, PA, 2004.

(12) Becke, A. D. *J. Chem. Phys.* **1993**, *98*, 5648.

(13) Lee, C.; Yang, W.; Parr, R. G. *Phys. Rev. B* **1988**, *37*, 785.

(14) Horng, M. L.; Gardecki, J. A.; Papazyan, A.; Maroncelli, M. *J. Phys. Chem.* **1995**, *99*, 17311.

(15) Bredenbeck, J.; Helbing, J.; Hamm, P. *Phys. Rev. Lett.* **2005**, *95*, 4.

(16) Pines, E.; Pines, D.; Ma, Y. Z.; Fleming, G. R. *ChemPhysChem* **2004**, *5*, 1315.

(17) Higuchi, S.; Tsuyama, H.; Tanaka, S.; Kamada, H. *Spectrochim. Acta* **1975**, *31A*, 1011.

(18) Andrews, S. S.; Boxer, S. G. *J. Phys. Chem. A* **2000**, *104*, 11853.
(19) Noda, I. *Appl. Spectrosc.* **1990**, *44*, 550.
(20) Noda, I.; Ozaki, Y. *Two-dimensional Correlation Spectroscopy: Applications in Vibrational and Optical Spectroscopy*; John Wiley & Sons: West Sussex, U.K., 2004.
(21) Schultz, P. W.; Leroi, G. E.; Popov, A. I. *J. Am. Chem. Soc.* **1996**, *118*, 10617.
(22) Wahab, A.; Mahiuddin, S. *J. Solution Chem.* **2005**, *34*, 537.
(23) Gast, K.; Siemer, A.; Zirwer, D.; Damaschun, G. *Eur. Biophys. J.* **2001**, *30*, 273.
(24) Starzyk, A.; Barber-Armstrong, W.; Sridharan, M.; Decatur, S. M. *Biochemistry* **2005**, *44*, 369.
(25) Hamm, P.; Lim, M.; Hochstrasser, R. M. *Phys. Rev. Lett.* **1998**, *81*, 5326.
(26) Kim, Y. S.; Hochstrasser, R. M. *Proc. Natl. Acad. Sci. U.S.A.* **2005**, *102*, 11185.